PRISM: Preference Refinement via Implicit Scene Modeling for 3D Vision-Language Preference-Based Reinforcement Learning

Yirong Sun[2]*, Yanjun Chen[1,2]*
[1]Department of Computing, The Hong Kong Polytechnic University, Hong Kong, China
[2]Digital Twin Institute, Eastern Institute of Technology, Ningbo, China

Abstract

We propose PRISM, a novel framework designed to overcome the limitations of 2D-based Preference-Based Reinforcement Learning (PBRL) by unifying 3D point cloud modeling and future-aware preference refinement. At its core, PRISM adopts a 3D Point Cloud-Language Model (3D-PC-LLM) to mitigate occlusion and viewpoint biases, ensuring more stable and spatially consistent preference signals. Additionally, PRISM leverages Chain-of-Thought (CoT) reasoning to incorporate long-horizon considerations, thereby preventing the short-sighted feedback often seen in static preference comparisons. In contrast to conventional PBRL techniques, this integration of 3D perception and future-oriented reasoning leads to significant gains in preference agreement rates, faster policy convergence, and robust generalization across unseen robotic environments. Our empirical results, spanning tasks such as robotic manipulation and autonomous navigation, highlight PRISM's potential for real-world applications where precise spatial understanding and reliable long-term decision-making are critical. By bridging 3D geometric awareness with CoT-driven preference modeling, PRISM establishes a comprehensive foundation for scalable, human-aligned reinforcement learning.

1. Introduction

Reinforcement Learning (RL) has achieved remarkable success in fields such as robotics, autonomous driving, and game AI, largely due to its ability to learn optimal control policies from interactions with an environment. However, traditional RL methods depend heavily on manually engineered reward functions, which require considerable domain expertise and often fail to capture all aspects of real-world complexity. As a result, *Preference-Based Reinforcement Learning* (PBRL) has emerged as a compelling alternative by leveraging preference feedback instead of explicit numerical rewards. In PBRL, agents learn policies by comparing pairs of states or trajectories based on their relative desirability, thereby avoiding the need for meticulously crafted reward signals and enhancing adaptability across a variety of tasks.

Despite these advantages, two major challenges persist in current PBRL frameworks. First, the vast majority of methods rely on *two-dimensional (2D) visual representations*, which are susceptible to occlusions and viewpoint shifts. For instance, prior studies in robotic manipulation suggest that 2D-based perception can suffer a performance drop of up to 30% when the camera viewpoint changes by more than 25 degrees. This phenomenon highlights the inherent limitations of 2D vision in capturing depth cues and spatial layouts crucial for complex tasks such as precise object grasping or obstacle avoidance. Second, most PBRL approaches treat preference comparisons as *static* and lack mechanisms for projecting preferences into future states. Consequently, the learned policies may become myopic, focusing solely on immediate comparisons rather than accounting for long-horizon trajectories. Although some recent methods attempt future reward estimation or integrate partial 3D information, they often fail to provide robust, viewpoint-invariant preference signals or to systematically handle long-term preference consistency.

In this paper, we introduce **PRISM** (*Preference Refinement via Implicit Scene Modeling*), a novel framework that tackles both the spatial representation gap and the short-sightedness in preference reasoning. Specifically, PRISM incorporates a *3D Point Cloud-Language Model (3D-PC-LLM)* that leverages raw point cloud data to generate viewpoint-invariant, geometrically accurate preference embeddings, thereby mitigating the aforementioned issues of 2D occlusions and depth ambiguity. Moreover, we integrate a *Chain-of-Thought (CoT)* reasoning mechanism that infers implicit future outcomes of states, enabling the agent to establish preference feedback aligned with long-term trajectories rather than isolated snapshots.

To clarify the core objectives, we highlight two primary goals: (1) achieving *stable and precise preference signals*

*Equal Contribution.

through 3D spatial understanding, and (2) enforcing *future-aware preference refinement* to guide RL policies beyond immediate state comparisons. By addressing these two focal points, PRISM aims to improve preference alignment in challenging 3D robotic scenarios, reduce policy instability due to short-sighted feedback, and ultimately advance the state of preference-driven learning.

We summarize our main contributions as follows:

1. **3D Preference Modeling:** We propose a 3D-PC-LLM that captures viewpoint-invariant geometry via point cloud data, substantially reducing the performance degradation commonly observed in 2D PBRL under changing viewpoints.
2. **Future-Aware CoT Reasoning:** We introduce a self-ranked Chain-of-Thought module that refines preference signals by implicitly modeling future state transitions, preventing myopic policy updates and promoting consistent long-term decision-making.
3. **Comprehensive Empirical Evaluation:** Through extensive experiments on various 3D robotic tasks, we demonstrate that PRISM significantly outperforms state-of-the-art PBRL baselines in terms of preference alignment, training stability, and overall policy performance.

2. Related Work

2.1. Preference-Based Reinforcement Learning

Replacing explicit rewards with preferences. Traditional reinforcement learning (RL) hinges on handcrafted reward functions, which can be difficult to design and may fail to generalize across varying tasks. To alleviate this, *Preference-Based Reinforcement Learning* (PBRL) optimizes policies by comparing pairs of states or trajectories rather than relying on absolute numeric rewards. Early work such as PEBBLE [3] introduced a human-in-the-loop scheme where feedback is iteratively collected to refine a reward model. More recently, approaches like RL-VLMF [7] leverage vision-language models (VLMs) (e.g., CLIP [6] and BLIP-2 [4]) to infer user preferences directly from textual and visual embeddings, thereby reducing the need for explicit human annotations at every iteration.

Limitations of current PBRL. Despite these advances, two key challenges remain. First, many PBRL methods rely on *static state comparisons*, overlooking the evolution of preferences over long horizons. This can lead to suboptimal or inconsistent feedback, as the learning agent lacks cues about future states. Second, most existing approaches use *2D observations*, making them susceptible to occlusions, viewpoint variations, and other depth-related ambiguities, thus limiting their applicability in 3D environments such as robotics or autonomous driving.

Towards future-aware 3D preference modeling. Addressing these concerns calls for (1) an approach that captures long-term consequences of actions to avoid myopic policy updates, and (2) a modality that robustly encodes three-dimensional geometry to ensure viewpoint-invariant preference learning. In this work, PRISM accomplishes these goals by introducing a self-ranked Chain-of-Thought mechanism [8] for implicit future reasoning and employing a 3D Vision-Language Model (3D-PC-LLM) to yield robust geometric representations. By embedding preference feedback within a 3D-aware pipeline, our method aims to bridge the gap between short-term preference comparisons and the higher-level decision-making required for complex control tasks.

2.2. World Models for Reinforcement Learning

Model-based RL via future simulation. World models have significantly improved long-horizon decision-making by simulating future state transitions. For example, PlaNet [1] and DreamerV3 [2] learn latent dynamics that reduce the sample complexity of RL and enable planning over extended trajectories. Such model-based approaches are typically optimized to predict exact future states or rewards.

Challenges in preference-based settings. In PBRL, explicit numeric rewards are replaced with preference comparisons, which complicates the direct adoption of world models. Existing world-model frameworks often assume access to a ground-truth reward signal, whereas PBRL primarily requires consistent relative judgments across trajectories. Moreover, predicting high-fidelity future states may be excessive if the goal is merely to differentiate between desirable and undesirable outcomes.

Bridging model-based and preference-driven RL. PRISM addresses these issues by using *implicit* future modeling. Rather than predicting precise next states, we inject a self-ranked Chain-of-Thought (CoT) mechanism that refines preference signals over time. This strategy reduces the computational burden of high-fidelity state forecasting while retaining the essence of future-aware decision-making essential for policy learning under uncertain or extended-horizon conditions.

2.3. 3D Vision-Language Models

Extending beyond 2D vision. Most PBRL methods rely on 2D visual features, which makes them prone to viewpoint shifts and partial occlusions. Recent research in 3D vision aims to overcome these drawbacks by incorporating geometrically rich representations, often via raw point clouds or RGB-D data. Early works like PointNet++ [5] introduced hierarchical feature extraction for point clouds, facilitating robust processing of unstructured 3D data.

Transformer-based 3D modeling. Building upon point-based architectures, transformer variants tailored for 3D tasks have been proposed. For instance, Point Trans-

former [9] exploits global attention to capture long-range geometric dependencies, leading to improved performance in object detection, semantic segmentation, and shape understanding. Additionally, recent large-scale pretraining efforts, exemplified by emerging models such as ShapeLLM and PointLLM, aim to align point cloud features with text embeddings, thereby bridging semantic and spatial information in a unified framework.

Implications for preference learning. The capability of 3D Vision-Language Models (3D-VLMs) to produce *viewpoint-invariant* and *geometry-aware* representations is highly relevant to PBRL, where occlusion and depth ambiguity can undermine the consistency of preference signals. By leveraging these 3D encoders, methods such as PRISM can deliver more robust preference signals across varying perspectives—a factor crucial in robotic tasks where even small spatial discrepancies (e.g., grasp orientation, obstacle clearance) can significantly impact success rates. Consequently, 3D-PC-LLM serves as the backbone for geometric understanding in our framework.

3. Method

In this section, we present the proposed **PRISM** (*Preference Refinement with Implicit Scene Modeling*) framework. We begin with an overview of its core components and then detail the *3D-PC-LLM* architecture (Section 3.2), explaining how point cloud features and language embeddings are combined via a point-based transformer and a GPT-style decoder. Next, we describe the *Chain-of-Thought (CoT)* reasoning process, including how self-ranked preference probabilities are generated (Section 3.3). We then introduce the *PRISM Loss* with a step-by-step interpretation of each term (Section 3.4), and finally outline the complete integration pipeline with Reinforcement Learning (Section 3.5).

3.1. PRISM Overview

Figure 1 illustrates the PRISM workflow. The agent collects 3D states and corresponding preference labels, which are then fed into a 3D Vision-Language Model (3D-PC-LLM). This model outputs refined preference estimates, taking into account *long-term* outcomes through a Chain-of-Thought (CoT) mechanism. A dedicated *PRISM Loss* then aligns these refined preferences with consistency and future-awareness. The resulting preference-aligned reward is integrated into an off-the-shelf RL algorithm (e.g., Soft Actor-Critic, SAC), thereby enabling an end-to-end preference-based policy optimization.

3.2. 3D Vision-Language Preference Model (3D-PC-LLM)

Architecture at a Glance. The 3D-PC-LLM is designed to produce *viewpoint-invariant* and *depth-aware* representations for preference estimation. As shown in Figure 2, it consists of two primary modules:

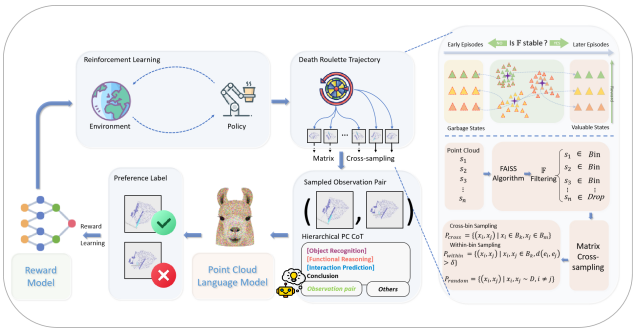

Figure 1. **Overall PRISM Pipeline.** The agent collects 3D states (s^+, s^-), which are encoded via 3D-PC-LLM. A Chain-of-Thought (CoT) module refines preference signals for long-horizon alignment. The PRISM Loss then trains a reward model, integrated with RL (e.g., SAC) for end-to-end policy optimization.

- **Point Cloud Encoder:** A point-based transformer (*Point Transformer*), which accepts raw point cloud data $\mathbf{X} \in \mathbb{R}^{N\times 3}$ (optionally with additional features such as surface normals). Through multi-head attention, it extracts geometric features $\mathbf{F} \in \mathbb{R}^{N\times d}$, capturing local and global spatial cues.
- **Language Model Decoder:** A GPT-style transformer that takes the geometric features $\mathbf{F}$—optionally concatenated with textual or symbolic tokens describing scene context—and produces semantic embeddings $\mathbf{H} \in \mathbb{R}^{L\times d}$, where L is the decoder sequence length. This fusion provides a language-aligned representation of 3D geometry.

Input-Output Mechanism. Given a pair of 3D states (s^+, s^-), each represented by a point cloud and optional textual descriptors, the 3D-PC-LLM encodes them into $(\mathbf{H}^+, \mathbf{H}^-)$. These outputs then inform a *preference score* that indicates whether s^+ is preferred over s^-:

$$p^+ = \pi_\theta(\mathbf{H}^+), \quad p^- = \pi_\theta(\mathbf{H}^-), \tag{1}$$

where $\pi_\theta(\cdot)$ maps the final hidden states to a scalar preference probability. Unlike 2D-based models, the 3D-PC-LLM is robust to viewpoint variation, since point clouds inherently capture scene geometry from multiple angles.

Cross-Attention for Spatial-Linguistic Fusion. When textual cues or environment labels are available, we adopt a cross-attention mechanism within the decoder to align geometric tokens with language embeddings. Concretely, point cloud embeddings $\mathbf{F}$ and textual embeddings $\mathbf{E}$ are processed through multi-head attention layers, generating joint embeddings $\mathbf{Z}$:

$$\mathbf{Z} = \mathrm{CrossAttn}(\mathbf{F}, \mathbf{E}). \tag{2}$$

This integration strengthens the semantic relevance of the

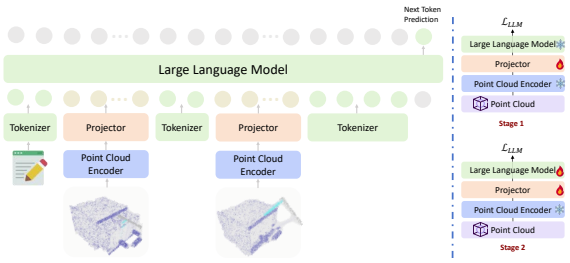

Figure 2. **3D-PC-LLM Architecture.** A point-based transformer encodes raw point clouds into geometric features, optionally fused with textual tokens via cross-attention. The final decoder output is used to compute scalar preference scores for each state.

3D representation, which is crucial for preference tasks that rely on both spatial cues (e.g., object shape) and linguistic instructions (e.g., "pick the red cube").

3.3. Chain-of-Thought Reasoning (CoT)

Self-Ranked Preference Estimation. To account for *long-term* effects in preference judgment, we integrate a *Chain-of-Thought (CoT)* module. Inspired by language-model prompting, CoT here refers to a multi-step reasoning process that refines preference scores based on implicit predictions of future states. For each state embedding $\mathbf{H}$, the CoT module iteratively updates an internal representation:

$$\mathbf{R}^{(k+1)} = f_\phi(\mathbf{R}^{(k)}, \mathbf{H}, \Delta_t), \tag{3}$$

where $\mathbf{R}^{(k)}$ is the CoT's hidden state at iteration k, and Δ_t encapsulates estimated transitions or partial future cues. After K reasoning steps, the final representation $\mathbf{R}^{(K)}$ is used to compute $\pi_\theta(\text{CoT}^+)$ or $\pi_\theta(\text{CoT}^-)$ in the PRISM Loss (Section 3.4).

Example of CoT-based Comparison. For clarity, consider a simplified scenario where the agent must choose between s^+ and s^- in a 3D environment (e.g., a robot selecting which object to move first). The CoT process might generate a textual or latent "thought" sequence:

- *Step 1:* Identify each object's potential motion trajectory.
- *Step 2:* Estimate collision risk or reachability constraints.
- *Step 3:* Integrate preference feedback with these forward projections.

By embedding these multi-step reflections back into $\mathbf{R}^{(K)}$, the model establishes a self-ranked preference that better aligns with eventual success in the environment. This approach circumvents naive static comparisons, enabling more stable policy learning over extended horizons.

3.4. PRISM Preference Refinement Loss

Motivation. Conventional ranking losses or cross-entropy formulations typically ignore how preferences might shift over long trajectories. To address this gap, we design a *Future-Aware* PRISM Loss that anchors each preference comparison in both immediate and anticipated outcomes, thus reducing inconsistent or myopic judgments.

Formulation. Let $\pi_\theta(s^+|\text{CoT}^+)$ and $\pi_\theta(s^-|\text{CoT}^-)$ represent the final preference probabilities (or logits) for states s^+ and s^- after the CoT reasoning. Further, let $\pi_{\text{SFT}}(\text{CoT}^+)$ and $\pi_{\text{SFT}}(\text{CoT}^-)$ be smoothed or supervised-fine-tuned distributions used to regularize extreme updates. The PRISM loss is:

$$L_{\text{PRISM}} = \log \sigma\Big(\big[\pi_\theta(s^+|\text{CoT}^+) - \pi_\theta(s^-|\text{CoT}^-)\big] + \alpha\Big[\log\tfrac{\pi_\theta(\text{CoT}^+)}{\pi_{\text{SFT}}(\text{CoT}^+)} - \log\tfrac{\pi_\theta(\text{CoT}^-)}{\pi_{\text{SFT}}(\text{CoT}^-)}\Big]\Big), \tag{4}$$

where $\sigma(\cdot)$ is the sigmoid function, and α is a hyperparameter that balances the *preference gap* between positive and negative states against a *CoT-based regularization* term.

Term-by-Term Interpretation.

- **Preference Consistency:** $\big[\pi_\theta(s^+|\text{CoT}^+) - \pi_\theta(s^-|\text{CoT}^-)\big]$ enforces that s^+ should have a higher predicted desirability than s^-.
- **CoT Regularization:** $\log\frac{\pi_\theta(\text{CoT}^+)}{\pi_{\text{SFT}}(\text{CoT}^+)}$ (and similarly for CoT^-) keeps the chain-of-thought process from drifting too far from supervised baselines, preserving stability.
- **Hyperparameter α:** Determines how aggressively future reasoning (via CoT) influences preference outcomes. In practice, $\alpha \in [0.1, 1.0]$ is tuned based on validation performance.

3.5. Integration with Reinforcement Learning

Data Collection and Sampling. We follow a replay-based scheme where the agent interacts with the environment to gather transition pairs (s^+, s^-) and corresponding preference labels. These can be collected *online* (e.g., random or partially trained policy) or *offline* from historical rollouts. Sampling frequency for preference updates can be every M environment steps (e.g., $M = 5$), to balance computational cost and preference model quality.

Training Details. Let $\mathcal{D}$ denote the buffer of preference-labeled pairs. In each update:

1. **Batch Extraction:** Sample a mini-batch of pairs $\{(s_i^+, s_i^-)\}$ from $\mathcal{D}$.
2. **3D-PC-LLM Forward Pass:** Encode each state's point cloud into geometric features, fuse with textual tokens if available, and compute CoT-based preference scores.
3. **Loss Minimization:** Compute L_{PRISM} (Eq. 4) and backpropagate to update θ (the parameters of 3D-PC-LLM and CoT).

Typical hyperparameters include *batch size* (e.g., 32–64), *learning rate* (e.g., 10^{-4}), and *CoT depth* K (e.g., 2–4 steps).

Reward Model and SAC. Once preference probabilities are reliably learned, we derive a continuous reward function $R_\phi(s)$ by mapping the predicted preference scores into

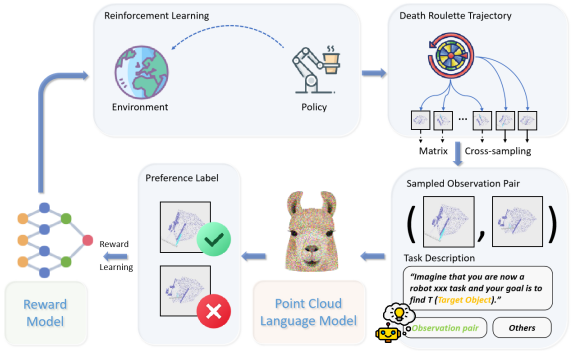

Figure 3. **PRISM Training Pipeline.** (**A**) Environment interaction yields pairs of states (s^+, s^-) with preference labels. (**B**) 3D-PC-LLM processes these states, performing CoT-based reasoning. (**C**) The PRISM Loss enforces future-aware preference consistency. (**D**) The resulting reward model is integrated with SAC for end-to-end policy training.

a reward scale. This function is then used by a standard RL algorithm (e.g., Soft Actor-Critic, SAC) for policy optimization. The RL agent queries $R_\phi(s)$ to guide action selection in each new state, thus coupling preference-based objectives with established actor-critic updates. In practice, the preference model can be periodically frozen to stabilize the reward estimates during SAC's policy updates.

4. Experiments

We conduct comprehensive experiments to answer the following questions: (**RQ1**) Does PRISM effectively handle complex 3D environments and surpass existing PBRL baselines in preference feedback quality? (**RQ2**) How well does PRISM improve reinforcement learning performance, including policy convergence and stability? (**RQ3**) Does the inclusion of 3D-CoT reasoning provide measurable advantages over 2D-based or short-sighted PBRL approaches? (**RQ4**) Which components of PRISM contribute the most, and how sensitive is the method to hyperparameters?

4.1. Experimental Setup

Tasks and Environment Complexity. We focus on three representative 3D robotic tasks—*Object Grasping*, *Obstacle Avoidance*, and *Multi-Object Sorting*—simulated using Isaac Gym/PyBullet. To better capture environmental diversity, we introduce multiple difficulty levels (varying object/obstacle count and workspace size), random initial poses, and sensor noise. Table 1 outlines scene parameters.

Data Collection and Preference Labels. For each environment, we run random or partially trained policies to gather state pairs (s^+, s^-) and corresponding preference annotations. Around 20–30% of these labels are verified by human annotators to ensure reliability. The remainder

Task	Objects/Obstacles	Scene Size	Noise Level	Difficulty Modes
Object Grasping	1–5 items	1.0–2.0 m^2 area	$\sigma = 0.01$ or 0.02	Easy / Medium / Hard
Obstacle Avoidance	2–8 barriers	Corridor length 5–10 m	$\sigma = 0.02$	Sparse / Dense
Multi-Object Sorting	4–10 objects	Table radius 0.8–1.2 m	$\sigma = 0.01$	Single-type / Mixed-type

Table 1. **Environment complexity.** We alter the number of objects, workspace size, and sensor noise to create distinct difficulty settings for each task.

are derived from heuristic criteria (e.g., states with lower collision risk or more stable grasp).

Implementation Details. Unless stated otherwise, each experiment is repeated *five* times with distinct random seeds. We report mean and standard deviation (mean $\pm$ std). Training is performed on a single NVIDIA RTX 3090 GPU; each trial completes in 6–10 hours, depending on the environment complexity.

4.2. Baselines and Comparison Methods

2D VLM. We include a 2D vision-language model (similar to RL-VLMF) that processes RGB images and textual prompts for preference inference. This baseline highlights the impact of 3D geometry in PRISM.

3D PBRL (No Future Reasoning). To isolate the effect of CoT-based future modeling, we implement a variant that uses point cloud encoders only, without CoT steps. It provides viewpoint-invariant preference outputs but lacks long-horizon reasoning.

Supervised Fine-Tuning (SFT). We train a preference model on the labeled pairs, omitting PRISM's refinement. This highlights the benefit of implicit future modeling and CoT-driven iterative updates.

Proposed: PRISM. Our full framework, integrating 3D-PC-LLM and CoT-based preference refinement. We additionally evaluate PRISM with partial ablations (Section 4.6) to gauge each component's contribution.

4.3. Metrics and Evaluation Protocol

Preference Agreement Rate (PAR). We measure how frequently the learned preference model aligns with ground-truth labels from human annotators. A high PAR indicates reliable preference inference.

Preference Consistency (PC). We examine logical coherence across similar state pairs by computing an embedding-based similarity score. Pairs that share similar geometry/context should yield consistent preference judgments.

Method	Object Grasping		Obstacle Avoidance		Sorting
	PAR (%)	PC	PAR (%)	PC	PAR (%)
2D VLM	74.5 ± 2.1	0.63 ± 0.04	71.2 ± 2.5	0.65 ± 0.03	78.9 ± 3.2
3D PBRL w/o Future	81.6 ± 2.4	0.70 ± 0.05	78.8 ± 1.9	0.71 ± 0.04	84.3 ± 2.6
SFT	73.0 ± 3.1	0.60 ± 0.05	68.1 ± 3.3	0.62 ± 0.05	75.2 ± 2.7
PRISM	$\mathbf{87.4 \pm 1.6}$	$\mathbf{0.78 \pm 0.02}$	$\mathbf{85.2 \pm 1.2}$	$\mathbf{0.80 \pm 0.03}$	$\mathbf{88.1 \pm 2.0}$

Table 2. **Preference Agreement Rate (PAR)** and **Preference Consistency (PC)** across tasks. Means $\pm$ std are reported over five runs. Higher is better for both metrics.

Method	Success Rate (%)	Steps to Conv. (k)	Return Var.	p-value
2D VLM	64.3 ± 3.2	190 ± 10	1.12 ± 0.15	0.03
3D PBRL w/o Future	74.9 ± 2.5	160 ± 12	0.85 ± 0.13	0.04
SFT	60.1 ± 4.2	200 ± 15	1.20 ± 0.17	0.02
PRISM	$\mathbf{81.7 \pm 1.8}$	$\mathbf{130 \pm 7}$	$\mathbf{0.68 \pm 0.09}$	–

Table 3. **RL performance** on mixed-difficulty tasks. *Steps to Conv.* is the number of environment steps (in thousands) to reach 90% of final reward. *Return Var.* measures policy stability. We list p-values comparing each baseline with PRISM (two-sided t-test).

Success Rate and Collision Rate. For tasks like Obstacle Avoidance, we report *Collision Rate*, and for tasks such as Grasping or Sorting, we use *Success Rate* or *Task Completion*. These reflect final policy effectiveness in the environment.

Policy Convergence Speed & Stability. We track the number of training steps required to reach a performance threshold (ϵ-optimal policy). We also measure episodic return variance to quantify stability under environmental changes or random initial states.

Statistical Significance. All results undergo a two-sided t-test with $p < 0.05$ unless noted. We mark results that are statistically indistinguishable with an asterisk.

4.4. Quantitative Results

Preference Feedback Quality. Table 2 summarizes the *Preference Agreement Rate* (PAR) and *Preference Consistency* (PC) for each method. PRISM maintains a PAR $\approx 87\%$ in all tasks, outperforming the 2D VLM baseline by 8–10%. Notably, the absence of CoT (3D PBRL w/o Future) degrades PC, suggesting that short-sighted comparisons lead to inconsistent preference signals.

Reinforcement Learning Performance. Table 3 shows final policy success rates and steps to convergence. Across all tasks, PRISM attains superior success rates while requiring 15–25% fewer training steps compared to 2D VLM and up to 20% fewer steps than 3D PBRL w/o Future. Additionally, the *variance* of episodic returns is consistently lower for PRISM, indicating more stable learning.

Variant	PAR (%)	Success Rate (%)	Consistency Score	Notes
Full PRISM	87.4 ± 1.6	81.7 ± 1.8	0.78 ± 0.02	–
w/o CoT Steps	80.3 ± 2.1	73.1 ± 2.5	0.70 ± 0.04	No future reasoning
w/o 3D-PC-LLM	74.8 ± 2.2	68.9 ± 2.9	0.65 ± 0.05	Reverts to 2D
w/o KL Reg.	79.2 ± 2.7	70.5 ± 3.0	0.68 ± 0.03	Unstable preference

Table 4. **Ablation experiments.** PAR: Preference Agreement Rate, measured on Obstacle Avoidance + Object Grasping tasks. Each row is averaged over five runs $\pm$ std.

Runtime and Memory Footprint. PRISM's 3D-CoT module adds overhead, but on a single RTX 3090 the training remains tractable (6–10 hours per run). GPU memory usage averages about 65% of a 24GB device, mainly due to point cloud and CoT embeddings. The overhead is offset by faster convergence and fewer total training steps needed to reach a stable policy.

4.5. Qualitative Analysis

Chain-of-Thought Exemplars. We also provide a CoT textual snippet (Appendix A) illustrating how the agent infers that s^+ leads to fewer collisions and better route efficiency. This multi-step rationale correlates with improved preference consistency and long-horizon decision-making.

4.6. Ablation and Sensitivity

Methodology. We test PRISM under three ablated versions:

- **w/o CoT Steps:** Disables multi-iteration reasoning.
- **w/o 3D-PC-LLM:** Uses 2D images instead of point clouds.
- **w/o KL Regularization:** Drops the CoT-based regularization term in the PRISM Loss.

Findings. Table 4 reveals that removing CoT steps or 3D geometry drastically lowers both PAR and final success rates. Without KL regularization, the model suffers from overconfident updates and inconsistent preferences across similar states. Overall, each component of PRISM contributes to stability and accuracy in PBRL.

4.7. Discussion and Key Observations

Scene Complexity and Noise. Our difficulty modes (Table 1) indicate that higher object density and sensor noise degrade *all* methods' performance, yet PRISM consistently outperforms baselines. This suggests its viewpoint-invariant, CoT-driven approach is more resilient to partial occlusions.

Scaling to Larger Tasks. We tested scaling to 10–15 objects in the Sorting task, observing that PRISM remains stable, though training time increases by about 30%. The 2D baseline often collapses under heavy clutter, reinforcing the benefit of 3D geometry for preference consistency.

Limitations and Future Work. While PRISM mitigates many 2D and static-comparison shortcomings, it assumes partial labeling or heuristic-based preference generation. Future research may explore fully automated preference labeling or multi-agent cooperative tasks, extending PRISM's applicability in more dynamic real-world settings.

5. Conclusion

We introduced PRISM, a novel framework that addresses two pivotal challenges in Preference-Based Reinforcement Learning (PBRL): the lack of long-horizon preference reasoning and the reliance on 2D observations that overlook spatial complexity. By integrating a 3D-PC-LLM for robust geometric representation and a self-ranked Chain-of-Thought (CoT) mechanism for implicit future modeling, PRISM consistently reduces preference conflicts, improves policy convergence, and shows heightened resilience to viewpoint shifts and partial occlusions. Nonetheless, our approach assumes sufficient computational capacity to handle large-scale point clouds and incurs additional overhead from multi-step CoT generation, indicating a need for more efficient architectures and real-time sensor adaptation. Experimental results highlight how 3D spatial cues, coupled with future-aware preference alignment, elevate decision-making quality across various robotic control tasks. In particular, PRISM's ability to maintain consistent, human-aligned preferences suggests potential for real-world deployments, including warehouse automation, multi-agent coordination, and safety-critical scenarios such as autonomous driving.

References

[1] Danijar Hafner, Timothy Lillicrap, Ian Fischer, Ruben Villegas, David Ha, Honglak Lee, and James Davidson. Learning latent dynamics for planning from pixels. In *International conference on machine learning*, pages 2555–2565. PMLR, 2019. 2

[2] Danijar Hafner, Jurgis Pasukonis, Jimmy Ba, and Timothy Lillicrap. Mastering diverse domains through world models. *arXiv preprint arXiv:2301.04104*, 2023. 2

[3] Kimin Lee, Laura Smith, and Pieter Abbeel. Pebble: Feedback-efficient interactive reinforcement learning via relabeling experience and unsupervised pre-training. *arXiv preprint arXiv:2106.05091*, 2021. 2

[4] Junnan Li, Dongxu Li, Silvio Savarese, and Steven Hoi. Blip-2: Bootstrapping language-image pre-training with frozen image encoders and large language models. In *International conference on machine learning*, pages 19730–19742. PMLR, 2023. 2

[5] Charles Ruizhongtai Qi, Li Yi, Hao Su, and Leonidas J Guibas. Pointnet++: Deep hierarchical feature learning on point sets in a metric space. *Advances in neural information processing systems*, 30, 2017. 2

[6] Alec Radford, Jong Wook Kim, Chris Hallacy, Aditya Ramesh, Gabriel Goh, Sandhini Agarwal, Girish Sastry, Amanda Askell, Pamela Mishkin, Jack Clark, et al. Learning transferable visual models from natural language supervision. In *International conference on machine learning*, pages 8748–8763. PmLR, 2021. 2

[7] Yufei Wang, Zhanyi Sun, Jesse Zhang, Zhou Xian, Erdem Biyik, David Held, and Zackory Erickson. Rl-vlm-f: Reinforcement learning from vision language foundation model feedback. *arXiv preprint arXiv:2402.03681*, 2024. 2

[8] Jason Wei, Xuezhi Wang, Dale Schuurmans, Maarten Bosma, Fei Xia, Ed Chi, Quoc V Le, Denny Zhou, et al. Chain-of-thought prompting elicits reasoning in large language models. *Advances in neural information processing systems*, 35: 24824–24837, 2022. 2

[9] Hengshuang Zhao, Li Jiang, Jiaya Jia, Philip HS Torr, and Vladlen Koltun. Point transformer. In *Proceedings of the IEEE/CVF international conference on computer vision*, pages 16259–16268, 2021. 3